DOI: https://doi.org/10.37434/tpwj2024.12.04

RESIDUAL STRESSES INDUCED BY FRICTION STIR WELDING OF HEAT STRENGTHENED ALUMINIUM 2219-T81 ALLOY PLATES

O.V. Makhnenko, O.S. Milenin, V.I. Pavlovsky, V.V. Savitsky, B.R. Tsaryk

E.O. Paton Electric Welding Institute of the NASU
11 Kazymyr Malevych Str., 03150, Kyiv, Ukraine

ABSTRACT

Friction stir welding (FSW) is a relatively new welding process that has already been widely used for joining structures in the aerospace industry, transport and shipbuilding. It is believed that, in comparison with traditional arc welding processes, FSW provides less heating of the joint metal and a reduction in the level of residual stresses and strains. In the work, the features of the distribution of residual stresses induced by FSW in the butt joint of the heat strengthened aluminium alloy are investigated, which is necessary for predicting the strength and service life of welded structures. A mathematical model was built to determine the residual stresses at FSW, and the effect of softening of the aluminium alloy during heating in welding on the residual stresses was considered. The comparison of calculated and experimental data on the distribution of residual longitudinal stresses in FSW specimens showed a satisfactory level of their correspondence. It is shown that the determined level of residual tensile stresses is close to the yield strength of the annealed metal.

KEYWORDS: aluminium alloy, friction stir welding, butt joint, residual stresses, mathematical modelling, experimental measurement

INTRODUCTION

Today, friction stir welding (FSW) technology is widely used to join different structures in the aerospace industry, transport and shipbuilding, etc. [1, 2]. To predict the reliability, service life, strength, and durability of FSW welded structures, an urgent task is to determine the residual stresses and strains [3, 4]. In view of the fact that the process of introducing FSW in the industry of developed countries began not so long ago — the last few decades — the issue of residual stresses and strains at FSW of various structural materials and alloys is still understudied. Therefore, there is no generally accepted idea of the level of maximum values and the nature of distribution of residual stresses and strains, and the existing data are often contradictory. For this purpose, the methods of experimental studies of the stress-strain state of the butt joint of aluminium alloy 2219-T81 plates under FSW welding heating were used [5], and the obtained distributions of residual stresses at FSW with the results of mathematical modelling were compared.

EXPERIMENTAL MEASUREMENT OF RESIDUAL STRESSES AT FSW

The experimental determination of residual stresses in specimens of aluminium alloy 2219-T81 joints, produced using FSW technology, was performed. The residual welding stresses were measured by the following methods:

1. By the method of cutting the welded joint metal into narrow longitudinal strips (templates) to relieve inner stresses in them and measuring the elastic strains obtained in this way (residual welding longitudinal stresses) [9]. For this purpose, a mechanical strain gauge on a 20 mm base was used (Figure 1) and a system of conical holes preliminary drilled on the upper and lower sides of the specimen in the cross-sections in the middle part of the specimens. The measurements were performed by means of a mechanical strain gauge on each measuring base (20 mm) before and after a complete cutting of the specimens into templates to completely relieve the residual stresses. After that, the elastic strain data of each measuring base was converted into residual welding stresses at

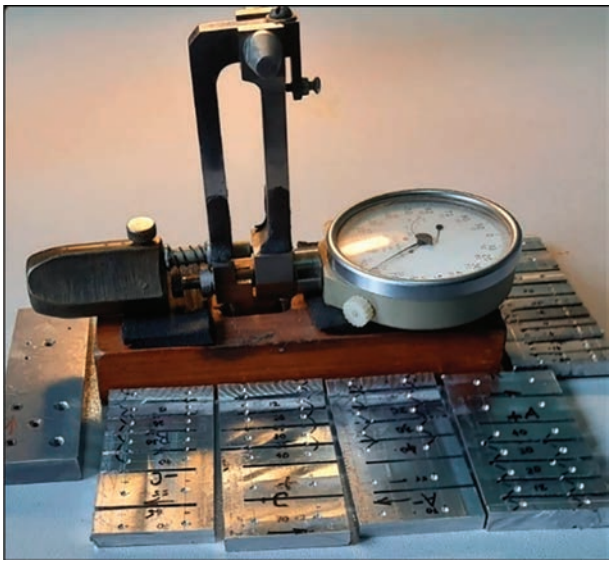

Figure 1. Appearance of mechanical strain gauge on a 20 mm base and cut-out parts of welded specimen (templates) with measuring bases (conical holes) for determination of residual stresses

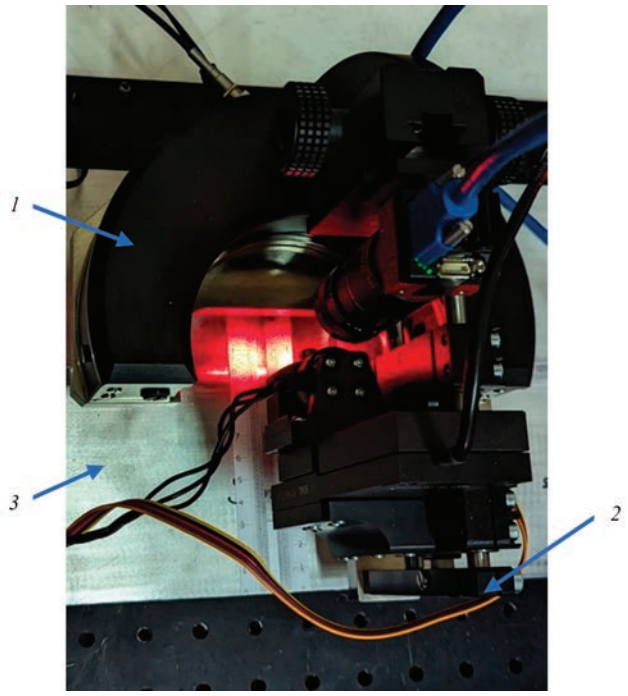

Figure 2. Appearance of ESPI-HD device for measurement of residual stresses

a set point of the specimen. For the aluminium alloy 2219, the modulus of elasticity E = 75000 MPa was used in the calculations.

2. By the hole method combined with the registration of displacements resulting from local stress relaxation using laser speckle interferometry (ESPI-HD method) (Figure 2). It does not require surface preparation and can be used to determine residual stresses on a base of 0.5–1.0 mm diameter and up to 1 mm depth. The measurements were performed in the following sequence: the speckle interferometer was placed on the welded joint, after which digital images were recorded, characterising the initial state of the surface before the hole was drilled. After the stress relaxation caused by drilling a 1.0 mm diameter and 0.5 mm depth through hole, another set of speckle images was recorded, that reflected the deformed state. Based on the obtained images, the displacement values in the specimen plane around the hole were calculated using the phase step method, which were used to determine residual stresses [10, 11]. The ESPI-HD method has demonstrated satisfactory agreement of stress measurement results with other traditional methods at the IIW Round-Robin test [12].

The specimen for measuring residual stresses represents a butt joint of two identical plates of 500 mm length, 300 mm width and 8 mm thickness. To measure residual elastic deformations, 26 measuring bases (52 holes) were used in the cross-section on both sides of the specimen (Figure 3).

The results of measuring residual longitudinal stresses in the specimen No. 1 in the central cross-section and in the specimen No. 2 in two cross-sections A and B (Figure 3) of the FSW butt joint specimen after

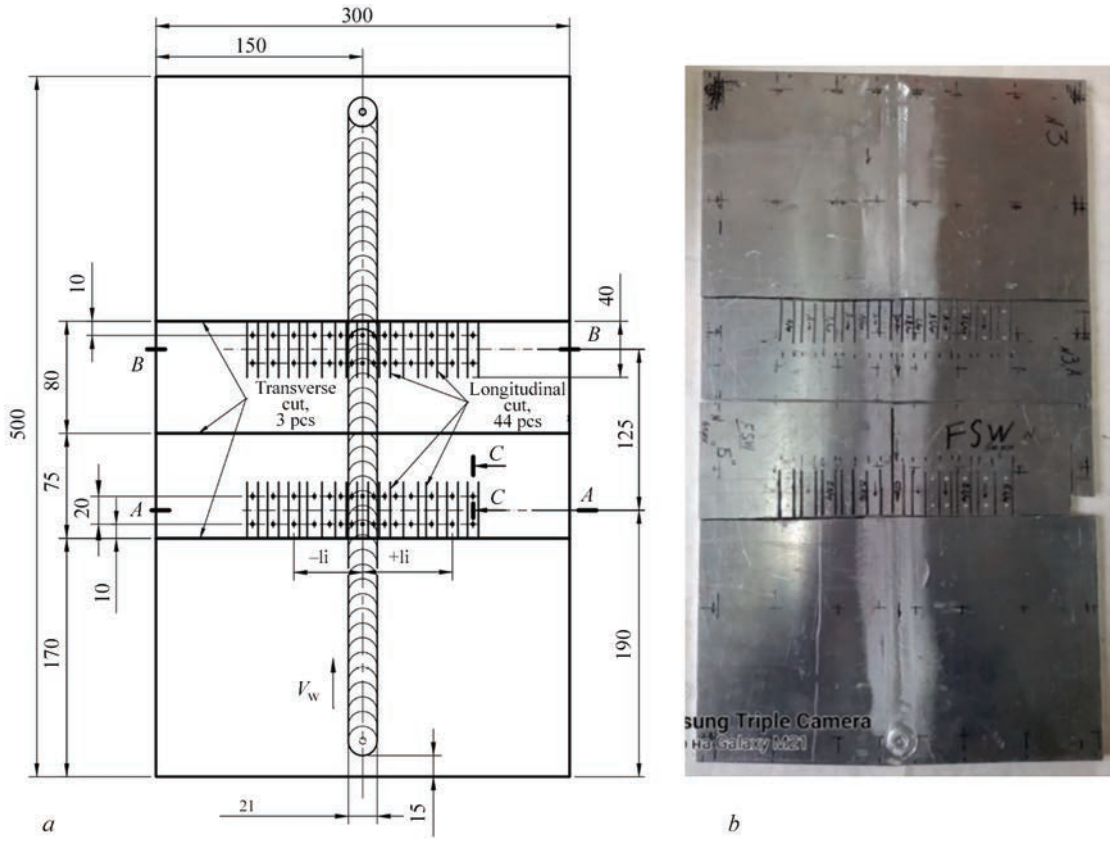

Figure 3. Layout of measuring bases (*a*) and appearance (*b*) of specimen (specimen No. 2) with dimensions of 500×300×8 mm of plates' butt joint according to the FSW technology

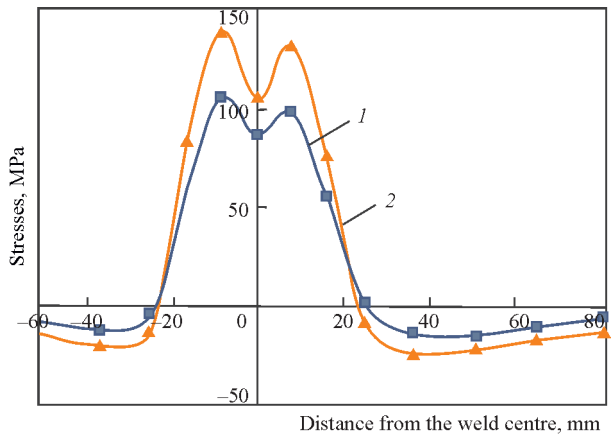

Figure 4. Residual longitudinal stresses in the central cross-section in the specimen No. 1 on the upper ($\sigma_{x,\ upper}$) (*1*) and lower ($\sigma_{x,\ lower}$) (*2*) sides of the specimen

a complete cutting of the material into longitudinal templates and measuring elastic deformations showed good repeatability of the results and a maximum level of tensile stresses of up to 180 MPa (Figures 4, 5). A significant difference was found between the level of residual longitudinal stresses on the upper and lower sides of the specimen. On the upper side, the level of measured stresses is noticeably lower: the maximum tensile stresses do not exceed 80–100 MPa, while on the lower side they reach 180 MPa. A significant bending component of the longitudinal stresses across the thickness is confirmed by the presence of a residual longitudinal deflection of the central part of the specimen of up to 2.5 mm.

The measurements by the speckle interferometry method (using drilling holes of 1 mm diameter) were carried out on the specimen No. 1 in two cross-sections: section 1 at a distance of 130 mm from the beginning of the weld and section 2 at a distance of 350 mm. In the section 1, the measurements were obtained on the upper and lower sides of the specimen, and in the section 2 — only on the lower side, in the zone of high tensile stresses. The measurement results showed (Figure 6, *a*) that the tensile longitudinal stresses on the upper side do not exceed 120–150 MPa, and on the lower side they reach 200–210 MPa. The remaining components of residual stresses have significantly lower values: transverse tensile stresses on the upper side do not exceed 20–25 MPa, and 50 MPa on the lower side (Figure 6, *b*).

The results of the stress state determination in the specimen No. 1 by two methods showed that at friction stir welding, the values of the maximum residual longitudinal stresses are quite high and close to the yield strength of the aluminium alloy A2219 in the annealed state (up to 150–180 MPa), i.e., taking into account the material softening in the welding heating

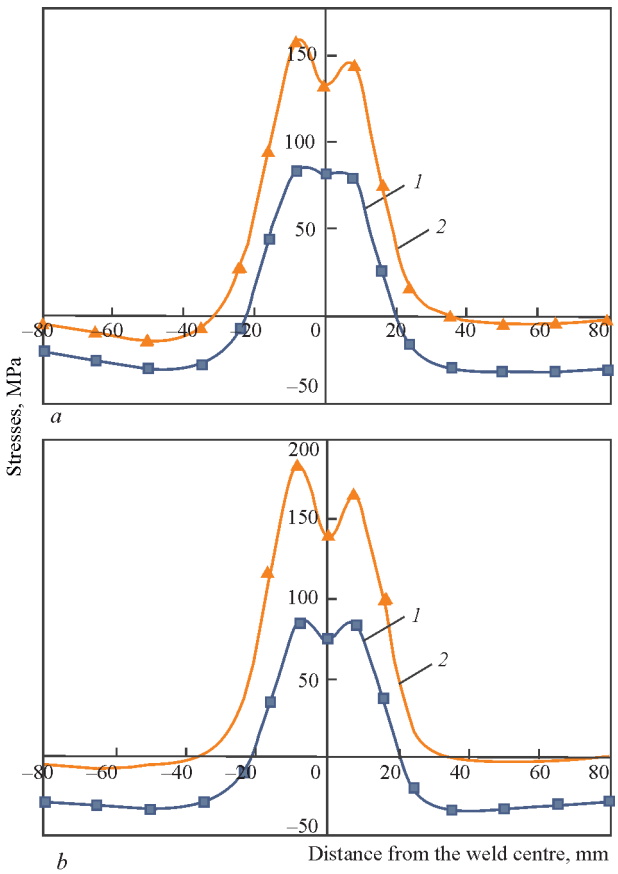

Figure 5. Experimental distributions of residual longitudinal stresses on both upper (*1*) and lower (*2*) sides of the weld specimen No. 2 in the cross-sections *A–A* (*a*) and *B–B* (*b*)

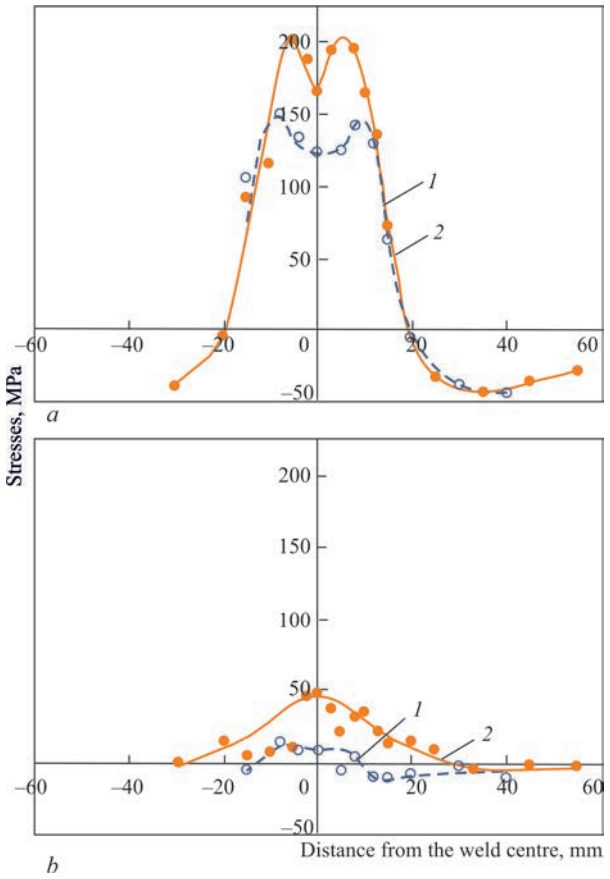

Figure 6. Results of measuring residual stresses by speckle interferometry in the specimen No. 1: *a* — longitudinal component; *b* — transverse component; *1* — upper side of the specimen; *2* — lower side of the welded specimen

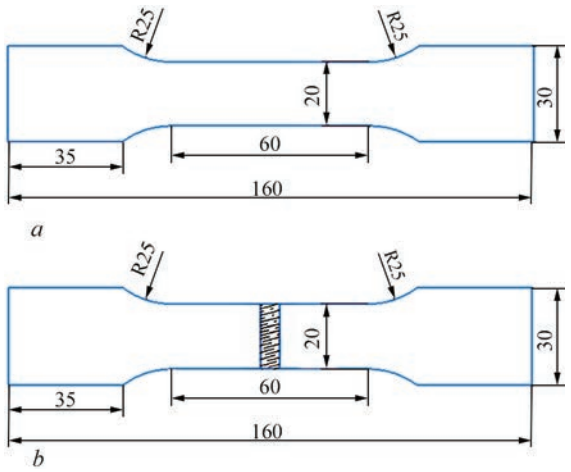

Figure 7. Diagrams of tensile specimens of the base metal (*a*) and welded joint metal (*b*)

zone. At the same time, residual stresses on the lower side of the specimen are significantly higher than those measured on the upper side: longitudinal stresses — by 20–30 %, transverse stresses — by 5 times.

MEASUREMENT OF MECHANICAL CHARACTERISTICS OF WELDED JOINT MATERIAL

The mechanical properties of welded specimens' material were studied. For uniaxial tensile tests, 10 tensile specimens were made from the base material (Figure 7, *a*) in two mutually perpendicular directions to determine the direction of rolled products. The welded joint metal is much less dependent on the direction of rolling due to the weld metal and HAZ recrystallization during the welding process. Thus, 10 specimens were used for these tests (Figure 7, *b*).

The test results showed that the influence of the rolling direction on the mechanical properties of welded specimen material does not exceed 4.5 %. This allows ignoring the material anisotropy when making the relevant expert assessments using the minimum

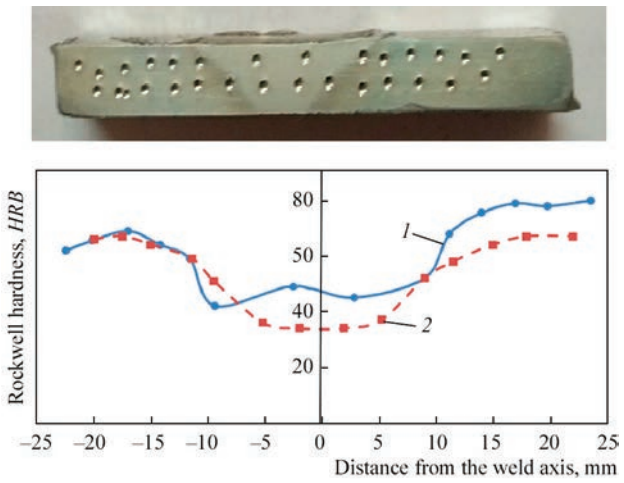

Figure 8. Rockwell hardness distribution in the FSW joint of the alloy A2219-T81 plates: *1* — upper side of the specimen; *2* — lower side of the specimen

average value ($\sigma_{0.2}$ = 370 MPa, E = 75.3 GPa). In addition, the process of metal recrystallization in the weld area has a significant impact, where a significant softening of the metal occurs: a decrease in the ultimate tensile strength σ_t to 44.4 % and in the true yield strength $\sigma_{0.2}$ to 63.4 % compared to the base material specimen along the rolled product.

According to the results of Rockwell hardness measurements in the cross-section of the test specimen (Figure 8), it was determined that in the welded joint zone in the HAZ, a material softening zone of ~20 mm width was observed, where the hardness characteristics were reduced by almost half, from an average of 70 to 35 *HRB*. This is also agreed with a decrease in the strength characteristics of the material for the alloy A2219-T81 in the HAZ, namely the yield strength from 350 to 160 MPa, determined as a result of mechanical tensile tests of the specimens.

COMPARISON WITH THE RESULTS OF MATHEMATICAL MODELLING OF FSW

For mathematical modelling of residual stresses at FSW of the aluminium alloy, the previously developed model [5] was used, which was supplemented by taking into account the effect of material softening in the weld zone and HAZ.

Temperature model:

$$c\rho\frac{\partial T}{\partial t}=\frac{\partial}{\partial x}\left(\lambda\frac{\partial T}{\partial x}\right)+ \\ +\frac{\partial}{\partial y}\left(\lambda\frac{\partial T}{\partial y}\right)+\frac{\partial}{\partial z}\left(\lambda\frac{\partial T}{\partial z}\right)+W(x,y,z,t), \quad (1)$$

where T is the temperature, °C; c is the specific heat capacity, J/kg·°C; ρ is the density, kg/m^3; λ is the thermal conductivity coefficient, W/m·°C; $W(x, y, z, t)$ is the power of volumetric heat generation, W/m^3.

The peculiarity of the developed model of the heating source at FSW is heat generation due to the friction of the tool relative to the joint material. The tool rotates around a vertical axis with a certain rotational velocity ω, rpm, and is pressed against the plates with an axial force P_n, Pa, which generates a heat flux into the joint material on the tool contact surface, W/m^2:

$$\lambda\frac{\partial T}{\partial n}=\mu P_n\omega r, \quad (2)$$

where μ is the friction coefficient; $r=\sqrt{(x-x_0-v_wt)^2+(y-y_0)^2}$ — is the distance of the considered contact point from the axis of the working tool rotation, $(x_0 + v_w t, y_0)$, v_w is the linear speed of the tool movement.

Then, the heat generation power Q, W, on the corresponding contact surfaces with an area S (Figure 9):

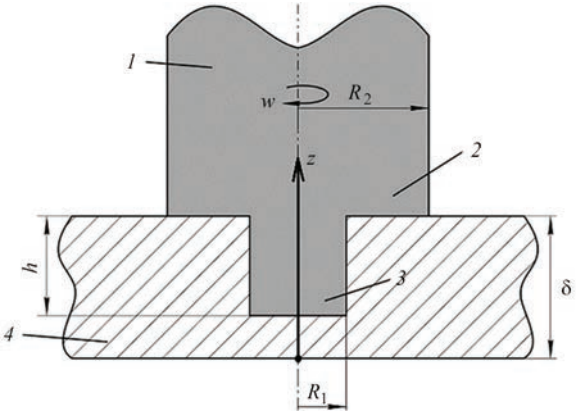

Figure 9. Schematic of FSW working tool: *1* — tool; *2* — shoulder; *3* — pin; *4* — plate

$$Q = \mu P_n \omega \pi \iint_s r dS; \quad (3)$$

arm

$$(z = \delta,\ R_1 < r < R_2),\ Q_1 = \frac{2\pi}{3}\mu P_n \omega (R_2^3 - R_1^3);$$

lateral surface of the pin

$$(\delta - h < z < \delta,\ r = R_1),\ Q_2 = 2\pi\mu P_n \omega R_1^2 h;$$

lower end surface of the pin

$$(z = \delta - h,\ 0 > r > R_1),\ Q_3 = \frac{2\pi}{3}\mu P_n \omega R_1^3,$$

where δ is the thickness of the plates to be welded, m; *h* is the length of the pin entering the material, m.

Accordingly, the power of volumetric heat generation $W(x, y, z, t)$, W/m³, consists of two components. The first is associated with heat generation in the volume V_1 on the upper side of the joining plates under the tool arm ($\delta - dz < z < \delta$, $R_1 < r < R_2$), dz is the size of the finite element, and the second one is in the volume of the pin V_2 ($\delta - h < z < \delta$, $0 > r > R_1$):

$$W(x, y, z, t) = W_1 + W_2;$$

$$W_1 = \frac{Q_1}{V_1} = \frac{\frac{2\pi}{3}\mu P_n \omega (R_2^3 - R_1^3)}{\pi (R_2^2 - R_1^2) dz} = \frac{2\mu P_n \omega (R_2^2 + R_2 R_1 + R_1^2)}{3(R_2 + R_1) dz}; \quad (4)$$

$$W_2 = \frac{Q_2 + Q_3}{V_2} = \frac{2\pi\mu P_n \omega R_1^2 h + \frac{2\pi}{3}\mu P_n \omega R_1^3}{\pi R_1^2 h} = 2\mu P_n \omega \left(1 + \frac{R_1}{3h}\right).$$

The model of thermoplastic deformation of the welded joint material at FSW is based on the assumption that the process of stirring the welded joint material occurs in the weld zone at a sufficiently high temperature and does not significantly affect the overall result of the formation and propagation of plastic deformations in the HAZ material and the weld behind the working tool. Therefore, plastic deformations and residual stresses are formed only as a result of the temperature gradient that occurs when the working tool moves as a source of volumetric heat generation [4]. The proposed mathematical model of thermoplastic deformation of the welded joint material at FSW is presented in more detail in [5].

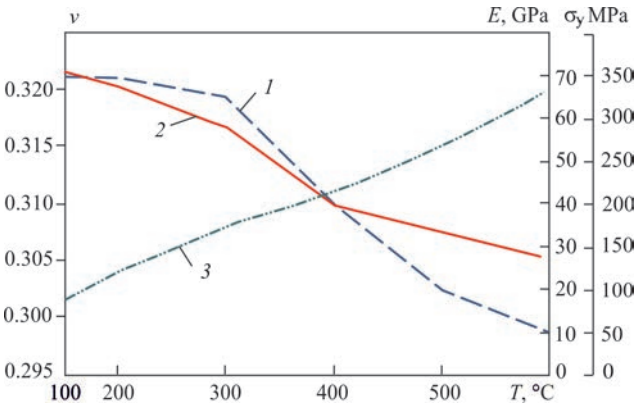

Figure 10. Mechanical properties of the alloy 2219-T81: *1* — $\sigma_y(T)$; *2* — $E(T)$; *3* — $\nu(T)$

In order to simplify the model, it was assumed that the value of the friction coefficient is independent of temperature and is approximately equal to the average value μ = 0.4 obtained for the aluminium alloy 2219 in the material temperature range of up to 400 °C [8].

Figures 10, 11 show the mechanical and thermophysical properties of the alloy 2219-T81 as a function of temperature [6], which were used in the mathematical modelling.

The analysis of the results of numerical experiments showed that among the factors that can to a greater or lesser extent influence the formation of residual stresses in the welded joint at FSW of aluminium alloys, softening of the material by welding heating has the greatest effect [7].

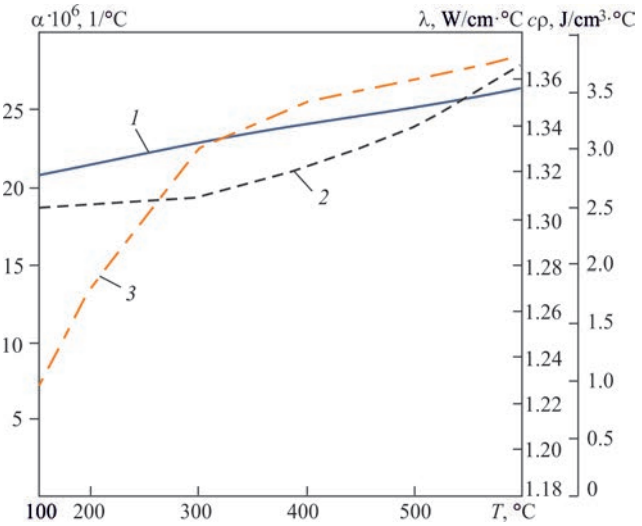

Figure 11. Thermophysical properties of the alloy 2219-T81: *1* — $\alpha(T)$; *2* — $c\rho\ (T)$; *3* — $\lambda(T)$

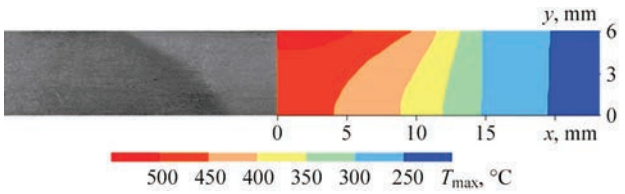

Figure 12. Comparison of the calculated distribution of the maximum temperatures in the cross-section of the FSW welded joint with the HAZ shape on the macrosection

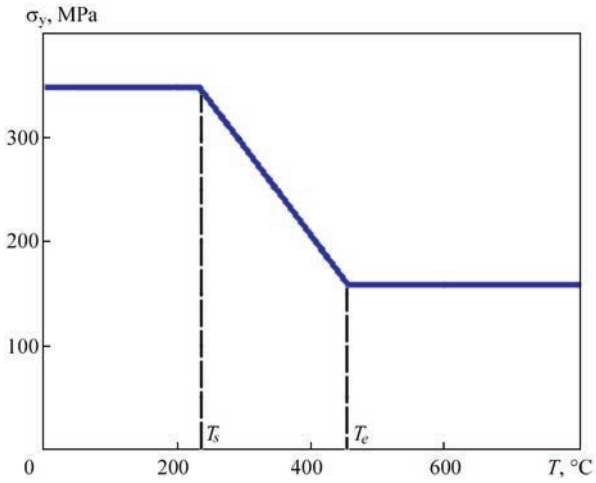

Figure 13. Dependence of the yield strength at 20 °C of the alloy A2219-T81 specimen on the maximum temperature in welding: T_s = 240 °C, T_e = 450 °C, σ_{soft} = 160 MPa, σ_y = 350 MPa

Comparison of the calculated distribution of maximum temperatures in the cross-section of the FSW welded joint of alloy A2219-T81 plates (Figure 12) with the results of hardness measurements (see Figure 8) showed that the width of the softening start zone of 40 mm corresponds to a temperature of T_s = 240 °C, and the zone of the maximum softening on the upper side with a width of ~20 mm and on the lower side with a width of 10 mm determines the temperature of softening end at the level of T_e = 450 °C of the material heating in welding.

The material softening parameters accepted in the model include the yield strength of the softened material σ_{soft} = 160 MPa, as well as the start temperature T_s = 240 °C and the end temperature T_e = 450 °C of softening (Figure 13). In the mathematical modelling of SSS at FSW, disregard of the material softening leads to a significant increase (by more than 30 %) in the maximum longitudinal residual stresses.

Comparing the calculation results and the experimental data obtained on the specimen No. 2, based on the distribution of residual longitudinal stresses at FSW (Figure 14), it can be stated that the nature of the distribution of the calculated residual stresses is close to the experimental one. In the centre of the welded joint, there is a zone of significant reduction in tensile longitudinal stresses, which is associated with the softening effect of the aluminium alloy. The width

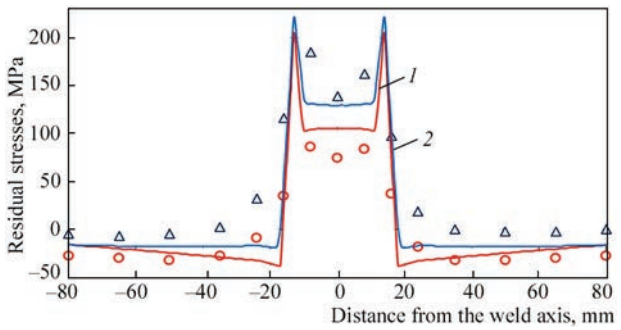

Figure 14. Comparison of experimental data with the results of mathematical modelling of the distribution of residual longitudinal stresses for the FSW specimen: experimental data: 0 — upper side of the specimen; Δ — lower side of the specimen; calculated data: *1* — upper side of the specimen; *2* — lower side of the specimen

of the tensile stress zone is approximately 36 mm (–18–+18 mm) and is the same for both experimental and calculated data.

The calculated stress distribution is characterised by sharper gradients and higher stress values in the weld zone. The smoother curve of the experimental residual stress distribution is associated with the sufficiently large step (8 mm) between the measurement points, which leads to an averaging of the stress values.

It is important that the experimental and calculated data are characterised by a significant difference between the stresses on the upper and lower sides of the welded joint — the residual longitudinal stresses are higher on the lower side. In terms of the absolute value of tensile stresses in the centre of the welded joint, this difference reaches 140 according to the experimental data and 130 MPa according to the calculation.

An assessment of the error of the calculated data for FSW shows that in the tensile stress zone (3 central points, –16–+16 mm), the mean square deviation from the experimental values on the lower side of the specimen is 21 %, and on the upper side it is up to 30 %. This error can be considered satisfactory, given the complex nature of the residual stress distribution.

CONCLUSIONS

1. For 8 mm thick specimens of welded butt joints made of the aluminium alloy A2219-T81 by friction stir welding, the measured level of tensile residual longitudinal stresses was quite high (up to 180 MPa), close to the yield strength of the aluminium alloy in the annealed state. At the same time, the residual stresses on the lower side of the specimen are higher than on the upper side (by about 20 %). The transverse tensile residual stresses are significantly lower: on the upper side they do not exceed 20–25 MPa, and on the lower side they do not exceed 50 MPa.

2. The result of mathematical modelling of residual stresses at FSW of aluminium alloys is significant-

ly influenced by considering the material softening model in the welding heating zone, the parameters of which include the yield strength of the softened material σ_{soft}, as well as the temperature range of the start T_s and end T_e of the softening effect. Disregard of the material softening leads to a significant increase (by more than 30 %) in the maximum longitudinal residual stresses.

REFERENCES

1. Hattel, J.H., Sonne, M.R., Tutum, C.C. (2015) Modelling residual stresses in friction stir welding of Al alloys— A review of possibilities and future trends. *Int. J. Adv. Manuf. Technol*., **76**, 1793–1805. DOI: https://doi.org/10.1007/s00170-014-6394-2
2. Poklyatskyi, A.G., Motrunich, S.I., Fedorchuk, V.Ye. et al. (2023) Mechanical properties and structural features of butt joints produced at FSW of aluminium alloys of different alloying systems. *The Paton Welding J.*, **4**, 3–10. DOI: https://doi.org/10.37434/tpwj2023.04.01
3. Feng, Z., Wang, X.-L., David, S.A., Sklad, P.S. (2007) Modelling of residual stresses and property distributions in friction stir welds of aluminium alloy 6061-T6. *Sci. and Technol. of Welding and Joining*, 12(**4**), 348–356. DOI: https://doi.org/10.1179/174329307X197610
4. Mohammad Riahi, Hamidreza Nazari (2011) Analysis of transient temperature and residual thermal stresses in friction stir welding of aluminum alloy 6061-T6 via numerical simulation. *Int. J. Adv. Manuf. Technol*., **55**, 143–152. DOI: https://doi.org/10.1007/s00170-010-3038-z
5. Tsaryk, B.R., Muzhychenko, O.F., Makhnenko,O.V. (2022) Mathematical model of determination of residual stresses and strains in friction stir welding of aluminium alloy. *The Paton Welding J*., **9**, 33–40. DOI: https://doi.org/10.37434/tpwj2022.09.06
6. Abdulrahaman Shuaibu Ahmad, Yunxin Wu, Hai Gong, Lin Nie (2019) Finite element prediction of residual stress and deformation induced by double-pass TIG welding of Al 2219 plate. *Materials*, 12(**14**), 2251. DOI: https://doi.org/10.3390/ma12142251
7. Makhnenko, O.V., Tsaryk, B.R. (2024) Consideration of material softening in the calculated determination of residual stresses at welding of aluminum alloy 2219-T81. In: *Proc. of 14th Int. Sci.-Pract. Conf. on Comprehensive Quality Assurance of Technological Processes and Systems*, *May 23–24, 2024, Chernihiv*, Chernihiv Polytechnic National University, NU Chernigivska Politekhnika, Vol. 2, 110–111.
8. Aziz, S.B., Dewan, M.W., Huggett, D.J. et al. (2016) Impact of friction stir welding (FSW) process parameters on thermal modeling and heat generation of aluminum alloy joints. *Acta Metal. Sin.*, **29**, 869–883. DOI: https://doi.org/10.1007/s40195-016-0466-2
9. Kasatkin, B.S., Kudrin, A.B., Lobanov, L.M. (1981) *Experimental methods for studying deformations and stresses.* Kyiv, Naukova Dumka [in Russian].
10. Lobanov, L.M., Pivtorak, V.A., Savitsky, V.V. et al. (2005) Express control of quality and stressed state of welded structures using methods of electron shearography and speckle-interferometry. *The Paton Welding J.*, **8**, 35–40.
11. Lobanov, L., Pivtorak, V., Savitsky, V., Tkachuk, G. (2014) Technology and equipment for determination of residual stresses in welded structures based on the application of electron speckle-interferometry. *Mat. Sci. Forum*, **768–769**, 166–173. DOI: https://doi.org/10.4028/www.scientific.net/MSF.768-769.166
12. Wohlfahrt, H., Nitschkepagel, T., Dilger, K. et al. (2012) Residual stress calculations and measurements — review and asessment of the IIW round robin results. *Weld. World*, **56**, 120–140. DOI: https://doi.org/10.1007/BF03321387

ORCID

O.V. Makhnenko: 0000-0002-8583-0163,
O.S. Milenin: 0000-0002-9465-7710,
V.I. Pavlovsky: 0000-0002-5441-3447,
V.V. Savitsky: 0000-0002-2615-1793,
B.R. Tsaryk: 0000-0002-8929-7722

CONFLICT OF INTEREST

The Authors declare no conflict of interest

CORRESPONDING AUTHOR

O.V. Makhnenko
E.O. Paton Electric Welding Institute of the NASU
11 Kazymyr Malevych Str., 03150, Kyiv, Ukraine.
E-mail: makhnenko@paton.kiev.ua

SUGGESTED CITATION

O.V. Makhnenko, O.S. Milenin, V.I. Pavlovsky, V.V. Savitsky, B.R. Tsaryk (2024) Residual stresses induced by friction stir welding of heat strengthened aluminium 2219-T81 alloy plates. *The Paton Welding J.*, **12**, 23–29.
DOI: https://doi.org/10.37434/tpwj2024.12.04

JOURNAL HOME PAGE

https://patonpublishinghouse.com/eng/journals/tpwj

Received: 15.08.2024
Received in revised form: 30.09.2024
Accepted: 27.12.2024